

Contents list available at CBIORE journal website

International Journal of Renewable Energy Development

Journal homepage: https://ijred.cbiore.id



Research Article

Low-carbon dispatch optimization of wind-solar-thermal-storage multi-energy system based on stochastic chance constraints and carbon trading mechanism

Hong Liu* , Yongwei Su , Kaijing Cai , Yingkang Mo

Guangdong Power Grid Corp, Dongguan Power Supply Bureau, Dongguan, 523000, China

Abstract. To improve the low-carbon economic performance of renewable energy-dominated power systems, a multi-energy coordinated optimization dispatch model for wind, solar, thermal, and storage systems considering uncertainties on both the supply and demand sides is proposed. This paper comprehensively considers the economic costs of thermal power unit operation, wind and solar power curtailment, energy storage operation, carbon trading and spinning reserve. The model incorporates a penalizing carbon trading mechanism and uses a stochastic chance-constrained approach to handle fluctuations in wind and solar power generation as well as uncertainties in load forecasting. The study, based on the IEEE 30-bus system, is solved using a stochastic simulation particle swarm optimization algorithm. Results show that after introducing the carbon trading mechanism, the system's carbon emissions were reduced by 8.35%, wind and solar curtailment penalties were reduced by 65.48%, and overall costs decreased by 14.94%. Additionally, the chance-constrained model effectively reduced the system's reserve capacity requirements, with reserve capacity decreasing by 31.84%, leading to a further reduction of 26.83% in overall costs. In the scenario of combined wind-solar-thermal-storage output, the wind and solar curtailment rate dropped to 7.37%, and carbon emissions decreased to 6474.69 tons. Through the "energy shifting" function, the energy storage system provided effective support during peak loads, further optimizing the dispatch outcomes.

Keywords: Wind-solar-thermal-storage system; Economic dispatch; Carbon trading; Chance-constrained programming; Stochastic simulation particle swarm optimization



@ The author(s). Published by CBIORE. This is an open access article under the CC BY-SA license (http://creativecommons.org/licenses/by-sa/4.0/).

 $Received: 22^{nd} \ Sept \ 2024; \ Revised: \ 5^{th} \ Dec \ 2024; \ Accepted: 14^{th} \ January \ 2025; \ Available \ online: 22^{nd} \ January \ 2025; \ Available \ online: 22^{nd} \ January \ 2025; \ Available \ online: 22^{nd} \ January \ 2025; \ Available \ online: 22^{nd} \ January \ 2025; \ Available \ online: 22^{nd} \ January \ 2025; \ Available \ online: 22^{nd} \ January \ 2025; \ Available \ online: 22^{nd} \ January \ 2025; \ Available \ online: 22^{nd} \ January \ 2025; \ Available \ online: 22^{nd} \ January \ 2025; \ Available \ online: 22^{nd} \ January \ 2025; \ Available \ online: 22^{nd} \ January \ 2025; \ Available \ Online: 22^{nd} \ January \ 2025; \ Available \ 22^{nd} \ Available \ 22^{nd} \ Available \ 22^{nd} \$

1. Introduction

Globally, the continuous growth in energy consumption has led to significant environmental impacts, especially the increase in greenhouse gas emissions, which has exacerbated climate change. To address this challenge, countries have set lowcarbon development goals, promoting the use of renewable energy and reducing dependence on fossil fuels. The clean energy transition of power systems has become a key global measure to combat climate change. The widespread adoption of renewable energy sources, such as wind and solar power, provides a critical opportunity to reduce carbon emissions, but their instability and volatility pose new challenges to the economic and stable operation of power systems (Njie et al. 2024; Takyi et al. 2024). How to optimize renewable energy integration and improve the low-carbon economic performance of systems while ensuring safety and stability has become a key research focus in the energy field (Gu et al. 2023; Liu et al. 2024; Wang et al. 2024).

Traditional power systems are dominated by fossil fuels, relying on the stable output of thermal power plants to maintain load balance (Wang *et al.* 2020). However, as the penetration of renewable energy increases, wind and solar power generation exhibit strong volatility and randomness, making traditional

dispatch models insufficient. To further enhance operational efficiency and renewable energy utilization, the concept of multi-energy coordinated optimization dispatch has emerged (Gu et al.2020). Coordinating wind and solar power with thermal power and energy storage systems can help mitigate the volatility of clean energy to some extent. Additionally, the introduction of carbon trading mechanisms has further promoted the development of low-carbon economic dispatch. By using market-based carbon regulation, power systems can achieve more efficient dispatch optimization, encouraging the broader application of renewable energy (Zhou et al.2023).

In recent years, as renewable energy has taken on an increasingly important role in global power systems, effectively dispatching volatile energy sources like wind and solar power has become a research focus in both academia and industry (Prawitasaria *et al.*2024). Many studies have explored various optimization dispatch methods aimed at improving the utilization of renewable energy and reducing dependence on fossil fuels.

In terms of addressing wind power uncertainty, researchers have proposed various mathematical modeling methods. Early studies widely employed Gaussian membership functions to describe wind power uncertainty. Using Gaussian functions, researchers could better model the volatility of wind power

* Corresponding author

Email: HongLiukk@163.com (H. Liu)

output and optimize dispatch strategies. For instance, Pandit *et al.* (Pandit. *et al.* 2015) proposed a dispatch method based on Gaussian membership functions, which significantly reduced system reserve capacity requirements and increased renewable energy utilization. Wang *et al.* (Wang *et al.* 2013) adopted an ascending half-trapezoidal membership function to describe wind power uncertainty, improving system robustness when dealing with wind power forecasting errors. In contrast, Ma, R. *et al.* (Ma *et al.* 2020) proposed a descending half-trapezoidal membership function to better handle the random fluctuations in wind power output. Although these methods partially address wind power uncertainty, their applicability often depends on specific scenarios and lacks broad generalization in complex systems.

Similar to wind power, the volatility of solar power also poses challenges to power system dispatch. Many researchers have attempted to jointly dispatch wind and solar power to take advantage of their complementary generation patterns. For example, some studies found that solar power generation during the day could compensate for low wind speeds, and vice versa. Yang et al. (Yang et al. 2021) proposed an optimized dispatch strategy based on wind-solar complementarity, effectively reducing wind and solar curtailment rates by leveraging their complementary characteristics. Wang et al. (Wang et al. 2022) further pointed out that coordinated optimization of wind and solar power can significantly reduce reliance on thermal power plants, thus lowering carbon emissions. These studies suggest that combining wind and solar power in dispatch strategies not only increases renewable energy utilization but also reduces system operational costs.

With the advancement of energy storage technologies, energy storage systems have become an increasingly flexible tool in power systems. Energy storage systems can store excess power from renewable sources and release it when generation is insufficient, providing a "peak-shaving and valley-filling" effect. Wang et al. (Wang et al.2021) proposed a multi-energy coordinated optimization dispatch method that integrates energy storage with wind and solar power, reducing load fluctuations and enhancing renewable energy utilization through the "energy shifting" function. Aunedi, M. et al. (Aunedi et al. 2023) further proposed that optimized energy storage configurations can reduce reliance on traditional thermal power plants and enhance system flexibility. These studies demonstrate that energy storage systems, as a key flexibility resource, can play a crucial role in highly uncertain renewable energy systems.

In recent years, driven by the urgent need to address climate change, carbon trading mechanisms have been introduced into power system dispatch as a market-based tool for carbon emission control. Carbon trading allows power companies to purchase carbon credits to compensate for excess emissions, thereby economically regulating carbon emissions. Ting et al. (Ting et al. 2018) proposed a low-carbon economic dispatch method based on carbon trading, achieving simultaneous optimization of system costs and carbon emissions through refined carbon management of power generation units. Rabe et al. (Rabe et al. 2019) found that the introduction of carbon trading mechanisms can effectively reduce carbon emission pressure in power systems, especially in scenarios with high penetration of renewable energy. Furthermore, He et al. (He et al. 2023) noted that in the coordinated dispatch of carbon trading mechanisms and energy storage systems, carbon emissions are significantly reduced, and overall economic performance is optimized.

To handle the random fluctuations of wind and solar power, chance-constrained programming methods have been widely applied in recent years. These methods use probabilistic descriptions of uncertainty, allowing the system to optimize dispatch strategies within a certain risk range. Ning et al. (Ning et al. 2021) proposed a chance-constrained power system dispatch model that handles wind power randomness at specified confidence levels. Zhan, S. et al. (Zhan et al. 2022) further noted that the chance-constrained model can effectively reduce system reserve capacity requirements and increase system flexibility. These methods exhibit strong robustness in high-penetration renewable energy scenarios but also face challenges related to computational complexity.

Despite the effectiveness of these methods in mitigating renewable energy volatility, several limitations remain (Liu *et al.* 2022). First, most studies focus on the optimization dispatch of individual energy forms like wind or solar, neglecting the potential of multi-energy coordinated dispatch in enhancing system stability. Additionally, many studies on carbon trading mechanisms focus on demand-side energy integration, without adequately considering the uncertainties in supply-side resources and renewable energy absorption. Current dispatch methods also struggle to balance economic efficiency and environmental benefits when facing complex uncertainties.

At present, most literature introduces carbon trading mechanisms, uses the integrated energy system to integrate multiple energy sources on the demand side, or only considers wind, fire, wind, fire and storage on the supply side to reduce carbon emissions; fewer literature is based on the resource endowment on the supply side, taking into account the uncertainty of clean energy and load, and adopts the synergy of wind, solar, fire and storage to balance the system's low-carbon economy and safe absorption of clean energy (Liu et al. 2022; Wu et al. 2022). Therefore, this study aims to develop a multienergy coordinated optimization dispatch model for wind-solarthermal-storage systems, introducing a penalizing carbon trading mechanism and using a stochastic chance-constrained approach to handle system uncertainties. The model is expected to improve the low-carbon economic performance of power systems, reduce carbon emissions, and enhance renewable energy absorption. Unlike existing research, this study considers the random volatility of renewable energy and introduces carbon trading to optimize carbon emission control. The stochastic chance-constrained approach effectively handles the uncertainties of wind, solar, and load, enhancing system reserve flexibility. Additionally, the proposed coordinated dispatch model for wind-solar-thermal-storage systems helps reduce overall operational costs, further promoting the development of low-carbon economic dispatch.

2. Research method

The wind, solar, thermal and storage integrated energy system constructed in this paper is at the regional level, which is based on meeting the electricity demand of the region and aims at minimizing the economic operation and carbon emissions of the system (Elahi Gol and Ščasný 2023). By optimizing the coordinated operation of various types of energy supply equipment and energy storage equipment, the system can achieve economic operation while taking carbon emissions into account. The system structure is shown in Figure 1.

2.1 Source of charge uncertainty model construction

Considering the impact of uncertainty, the actual value of wind power, photovoltaic output and load can usually be expressed

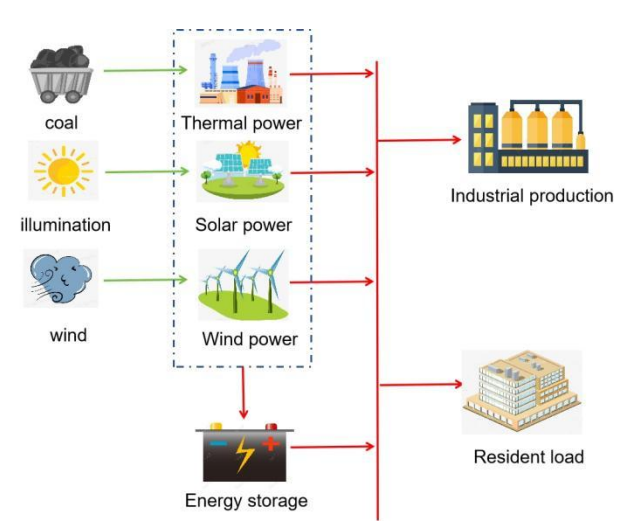


Fig. 1 Schematic diagram of regional integrated energy system

as the determined prediction value plus the uncertain prediction error, namely:

$$P_{wr,t} = P_{wpre,t} + \varepsilon_{w,t} \tag{1}$$

$$P_{gr,t} = P_{gpre,t} + \varepsilon_{g,t}$$
 (2)

$$P_{lr,t} = P_{lpre,t} + \varepsilon_{l,t}$$
 (3)

Where, $P_{wr,t}$, $P_{gr,t}$, $P_{lr,t}$ are the actual values of wind power, photovoltaic and load, respectively; $P_{wpre,t}$, $P_{gpre,t}$, $P_{lpre,t}$ are wind power, photovoltaic and load forecast power respectively $\varepsilon_{w,t}$, $\varepsilon_{g,t}$, $\varepsilon_{l,t}$ are wind power, photovoltaic and load prediction error power.

According to the central limit theorem, the uncertainty error follows a normal distribution, namely:

$$\sigma_{w,t} = 0.2P_{wpre,t} + 0.02P_{wr} \tag{4}$$

$$\sigma_{g,t} = 0.2P_{gpre,t} + 0.02P_{gr}$$
 (5)

$$\sigma_{l,t} = 0.03 P_{lpre,t} \tag{6}$$

Where, $\sigma_{w,t}$, $\sigma_{g,t}$, $\sigma_{l,t}$ are the standard deviation of normal distribution with mean of 0; P_{wr} and P_{gr} are the rated installed capacity of wind power and photovoltaic power, respectively.

Wind speed, light intensity and load are affected by the uncertainty of natural conditions and electricity consumption habits, making it difficult to accurately predict (Jin *et al.* 2022). The expression considering the uncertainty of landscape load is formula (7) - -formula (8).

Power balance:

$$\begin{split} P_{L,t} + P_{E,chr,t} - \left(P_{w,t,t} - P_{qw,t} \right) - \left(P_{gr,t} - P_{qb,t} \right) - \\ \sum_{i=1}^{n} P_{G,i,t} - P_{E,dis,t} &= 0 \end{split} \tag{7}$$

Rotate the standby balance:

$$P_{lr,t} + \sum_{t=1}^{T} P_{E,chr,t}^{max} - (P_{ww,t} - P_{qw,t}) - (P_{gr,t} - P_{qg,t}) - \sum_{i=1}^{n} P_{Gi}^{max} - \sum_{t=1}^{T} P_{E,dis,t}^{max} \le 0$$
(8)

Where, $P_{E,chr,t}$, $P_{E,dis,t}$ are the energy storage charging and discharge power respectively; $P_{qw,t}$, $P_{qg,t}$ are air abandon and light abandon, respectively; $P_{G,i,t}$ is the power at time t of the i thermal power unit; P_{Gi}^{max} is the maximum power of the first i thermal power unit; $P_{E,chr,t}^{max}$, $P_{E,dis,t}^{max}$ are respectively the maximum charge and discharge amount of energy storage at time t; T is the total number of daily scheduling periods, and T =24

2.2 Chance-constrained model processing

The chance constraint satisfies the constraint in the form of probability, namely that the scheduling result can be beyond the constraint range to some extent, but the probability of allowing the constraint to hold is not less than the previously set confidence level (Huang *et al.* 2022).

The general form of the opportunity constraint planning model is:

$$\begin{cases} \min\{(x,\xi) \\ \text{s.t.} P_r\{g_i(x,\xi) \leq \alpha\}, j = 1,2,...,k \end{cases}$$
(9)

Bring equation (1) - -equation (8) into equation (9), and the opportunity constraint model available for scheduling is:

$$\begin{aligned} & \min P_{r} \left\{ P_{lpre,t} + \epsilon_{l,t} + P_{E,chr,t} - \left(P_{wpre,t} + \epsilon_{w,t} - P_{qw,t} \right) - \left(P_{gpre,t} - \epsilon_{g,t} - P_{q\xi,t} \right) - \sum_{i=1}^{n} P_{G,t,t} - P_{E,dis,t} = 0 \right\} \geqslant \alpha \end{aligned}$$

$$(10)$$

$$\min P_{r} \left\{ P_{lpre,t} + \varepsilon_{L,t} + \sum_{t=1}^{T} P_{E,chrts}^{max} - \left(P_{wpre,t} + \varepsilon_{w,t} - P_{qw,t} \right) - \left(P_{gpre,t} - \varepsilon_{g,t} - P_{qg,t} \right) - \sum_{i=1}^{n} P_{Gi}^{max} - \sum_{t=1}^{T} P_{E,dis,t}^{max} \leq 0 \right\} \geqslant \beta$$

$$(11)$$

Where, α , β are the confidence level of power balance and rotating standby balance, respectively.

In this paper, Monte Carlo simulated stochastic chance constraint method. By stochastic Monte Carlo simulation with random variables, the results need to satisfy the confidence level.

2.3 System carbon trading cost model

According to the residential electricity habit, the load curve within 1 d is "double peaks" in the morning and evening, while the wind power is often at night and early morning, the daytime output is small, and the output of the wind power and load have obvious reverse peak regulation characteristics in the daytime, and the output at night and early morning is almost zero. Individual grid connection will increase the peak and valley difference of net load, and then increase the peak regulation pressure of thermal power units, and the utilization rate of wind power and photovoltaic is not high (Lou et al. 2022). Using the complementarity of combined grid connection in scenery time, the volatility of power generation can be gentle to a certain extent. The "energy time shift" of energy storage stores the electric energy when the wind output is high but the load demand is low. When the output is low and the load demand is high, the electric energy is released to further smooth the output curve and solve the reverse peaking.

Compared with the moderate carbon reduction mode of setting carbon quota, the carbon trading mechanism is a market trading method for the carbon rights of power producers according to the Kyoto Protocol. On the principle of economic leverage, it is a scientific combination of high pollution, low cost and low pollution and high cost, so as to achieve the purpose of reducing carbon emissions.

2.3.1. The actual carbon emissions

A large amount of CO₂ is generated during the operation of conventional coal-fired units, and the parts below or beyond the carbon emission quota can be sold for carbon rights. Although CO₂, the uncertainty of wind power and photovoltaic causes the grid. This paper considers the increase of standby carbon emissions caused by wind power, photovoltaic and load uncertainty, which is regarded as the carbon emission of wind load, namely:

$$\begin{cases} E_{Gt} = \sum_{i=1}^{n} \delta_{i} P_{Gi,t} \\ E_{wt} = \sum_{i=1}^{n} \delta_{i} P_{wb,t} \\ E_{gt} = \sum_{i=1}^{n} \delta_{i} P_{gb,t} \\ E_{lt} = \sum_{i=1}^{n} \delta_{i} P_{lb,t} \end{cases}$$

$$(12)$$

$$E_{pt} = E_{Gt} + E_{wt} + E_{gt} + E_{lt}$$
 (13)

Where, E_{Gt} , E_{wt} , E_{gt} , E_{lt} are the actual carbon emission at time t of thermal power, wind power, photoelectric and load respectively; P_{Gi,t} ,P_{wb,t} ,P_{gb,t} ,P_{lb,t} are the pre-day dispatching output of the i thermal power, wind power, photoelectric and load standby time t.

2.3.2 Carbon emission right quota

At present, China is in the early stage of the implementation of the low-carbon emission reduction policy. Most of the carbon trading quotas are allocated for free, so the carbon emission sources can obtain the corresponding carbon emission quotas as follows:

$$\begin{cases} D_{Gt} = \lambda \sum_{i=1}^{n} P_{Gi,t} \\ D_{wt} = \lambda \sum_{i=1}^{n} P_{wr,t} \\ D_{gt} = \lambda \sum_{i=1}^{n} P_{gr,t} \\ D_{lt} = \lambda \sum_{i=1}^{n} P_{lb,t} \end{cases}$$

$$(14)$$

$$E_{at} = D_{Gt} + D_{wt} + D_{gtt} + D_{ltt}$$
(15)

Where, D_{Gt}, D_{wt}, D_{gt}, D_{lt} are the carbon emission quota at time t for thermal power, wind power, photovoltaic power and load reserve respectively, \(\lambda\) is Distribution amount of carbon emission per unit of electricity by using the base line method.

2.3.3 Carbon trading costs

According to the relationship between the actual emission of carbon source and the carbon quota and the purchase of carbon rights, the carbon trading costs with punishment are mainly three: the purchase cost of carbon rights, carbon income and excessive emission punishment (Yan et al. 2022). The calculation formula is:

$$C_{co_{2},t} = \begin{cases} K_{pt}(E_{pt} - E_{qt}), E_{pt} \leq E_{qt} \\ K_{pt}(E_{pt} - E_{qt}), E_{qt} \leq E_{pt} \leq E_{ct} + E_{qt} \\ K_{pt}E_{Ht} + K_{ft}(E_{pt} - E_{ct} - E_{qt}), E_{pt} \geqslant E_{ct} + E_{qt} \end{cases}$$
(16)

$$E_{ct} = \mu E_{at} \tag{17}$$

Where, Ept, Eqt, Ect are respectively the actual carbon source emissions, carbon emission quota and market carbon emission right purchase; $C_{co_2,t}$ is the cost of system at time t; K_{pt} , K_{ft} are the carbon trading price at time t and the excess penalty price, respectively; μ is purchase of margin for carbon rights.

2.4 System operation objective function

As a traditional controllable power source, thermal power unit plays an important role in the stable and safe operation of the power grid; due to the influence of natural conditions such as wind speed and light intensity, and its large-scale grid connection, it is difficult to match the load demand, which will cause a large amount of wind and light abandonment (Gao et al. 2024). This paper considers the economic costs of thermal power unit operation, wind and light abandonment, energy storage operation, carbon trading and rotary reserve (Jin et al. 2023).

Comprehensive system cost is:

$$F_{c} = \sum_{t=1}^{T} \left(C_{Gi,t} + C_{qf,t} + C_{qp,t} + C_{ess,t} + C_{ri,t} + C_{co_{2},t} \right)$$
 (18)

Where, F_c is the comprehensive cost of the system; $C_{Gi,t}$, $C_{qf,t}$, $C_{qp,t}$, $C_{ess,t}$, $C_{ri,t}$ are respectively the power generation cost of thermal power unit, penalty cost of wind and light abandonment, energy storage cost and standby machine. The details are as follows:

$$C_{Gi,t} = \sum_{i=1}^{n} (a_i P_{gi,t}^2 + b_i P_{g,t} + c_{i,t})$$

$$C_{q,t,} = D_{cw} P_{qw,t}$$
(19)

$$C_{q,t} = D_{cw} P_{qw,t}$$
 (20)

$$C_{qg,t} = D_{cg}P_{qg,t} \tag{21}$$

$$C_{ess,t} = D_{ce} (P_{E,chr,t} + P_{E,dis,t})$$
 (22)

$$C_{r,t} = D_s(r_{i,t}^d + r_{i,t}^u)$$
 (23)

Where, D_{cw} and D_{cg}are the penalty coefficient for abandoning wind and light; Dce is the energy storage cost coefficient; Dsis the rotating spare cost coefficient; $r_{i,t}^d$, $r_{i,t}^u$ are positive and negative rotation reserve capacity at time t, respectively.

2.5 System operation constraints

Thermal power unit constraints

(1) The output constraint is:

$$P_{Gi}^{\min} \leqslant P_{Gi,t} \leqslant P_{Gi}^{\max} \tag{24}$$

(2) The climbing constraint is:

$$-R_{di} \cdot \Delta T \leqslant P_{G,it+1} - P_{Gi,t} \leqslant R_{ui} \cdot \Delta T \tag{25}$$

Where, R_{di} ,R_{ui} are the upward and downward climbing rates of i thermal power units respectively.

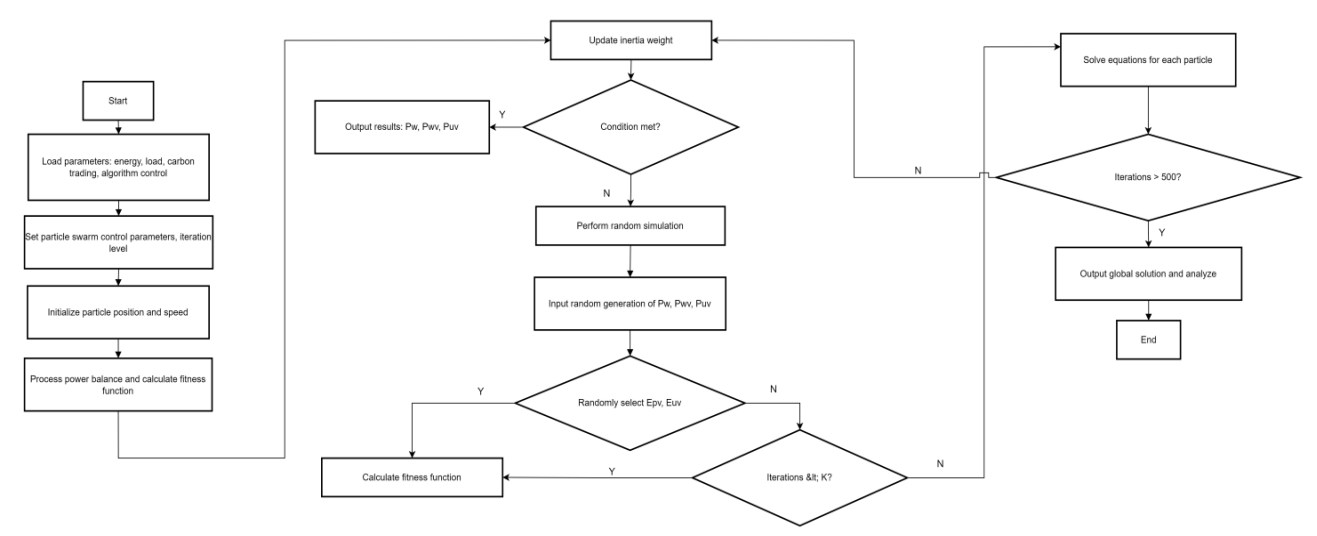


Fig. 2 Stochastic simulation of the particle swarm algorithm

Wind power constraints

(1) The output constraint is:

$$0 \leqslant P_{w,t} \leqslant P_{wr} \tag{26}$$

(2) The air abandon volume constraint is:

$$0 \leqslant P_{\text{qw,t}} \leqslant P_{\text{wr,t}} \tag{27}$$

Photovoltaic constraints

(1) The output constraint is:

$$0 \leqslant P_{\sigma r t} \leqslant P_{\sigma r} \tag{28}$$

(2) The constraint of light discard amount is:

$$0 \leqslant P_{qf,t} \leqslant P_{fr,t} \tag{29}$$

Energy storage constraints

(1) The energy storage quantity is:

$$P_{E,chr,t} = P_{E,t} \cdot \Delta t \cdot \eta_c \tag{30}$$

$$P_{E,dis,t} = P_{E,t} \cdot \Delta t / \eta_d \tag{31}$$

$$E_{t} = \rho E_{t-1} - P_{E,chr,t} - P_{E,dis,t}$$
 (32)

where, η_c , η_d are respectively the charge and discharge efficiency; ρ is The power loss rate; E_t is the equivalent power supply of energy storage.

(2) Power constraint is:

$$P_{E,cm,t}^{max} + P_{E,t}^{up} \leqslant P_{ess,t} \leqslant P_{E,dis,t}^{max} - P_{E,t}^{dw}$$
(33)

$$P_{E,drr,i} \cdot P_{E,dis,s} = 0 \tag{34}$$

(3) The standby constraint is:

$$P_{E,t} + P_{E,t}^{up} \leqslant \frac{E_{t-1} - \sum_{t=1}^{T} E_{t}^{max}}{\Lambda t} \leqslant P_{E,t} + P_{E,t}^{dw}$$
 (35)

Where, $P_{E,t}^{up}$, $P_{E,t}^{dw}$ are the positive and negative reserves for the equivalent power supply at time t; $P_{E,t}$ is the equivalent power supply power of energy storage at time t.

(4) The capacity constraint of the state of charge is:

$$E_{\min} \leqslant E_{t} \leqslant E_{\max} \tag{36}$$

Where, E_{min} , E_{max} are the minimum and maximum energy storage, respectively.

3. Case Study Analysis

3.1 Model Solution

Particle Swarm Optimization (PSO) has advantages such as fewer parameters, fast convergence speed, and better selection of global optimal solutions. It is highly capable of solving nonlinear and multi-peak problems (Zhang *et al.* 2020). Since the power balance and spinning reserve balance constraints in this study involve random variables, a combination of stochastic simulation and PSO is adopted, referred to as the Stochastic Simulation Particle Swarm Optimization (SSPSO). The flowchart of this process is shown in Figure 2.

3.2 Case Parameters

The IEEE 30-bus system is used as the case study for analysis, with a dispatch period of 24 hours and a time interval of 1 hour. The cost coefficients and unit emission intensity of the thermal power units, as well as the parameters of the energy storage system, are listed in Table 1. The wind power, solar power generation, and load forecasting parameters are shown in Figure 3. The benchmark emission quota for unit power generation is set at 0.798 tons/MWh, and the carbon trading price is 120 yuan/ton. The confidence levels for the chance constraints are set to $\alpha=100\%$ and $\beta=97\%$, and the carbon credit purchase margin is 0.3. Additionally, the penalty cost for wind and solar curtailment is 500 yuan/MW, and the cost for reserve capacity is 200 yuan/MW. The algorithm parameters are set with learning factors c1=1.3 and c2=1.492, a maximum iteration count of 500, and 3,000 stochastic simulation iterations (Liu et al. 2023).

3.3 Case Study Results Analysis

3.3.1 Impact of Carbon Trading and Chance Constraints on the System

The energy storage parameters are shown in Table 1. To verify the effectiveness of introducing carbon trading and chance constraints in the economic objective function on system

Table 1Energy storage parameter

Parameter	Value
Maximum charging/discharging power (MW)	20/20
Maximum/minimum energy (MWh)	150/10
Charging/discharging efficiency (%)	85/95
Self-discharge rate of the battery $\rho/\%$	0.996
Energy storage cost [yuan/MWh]	83.3

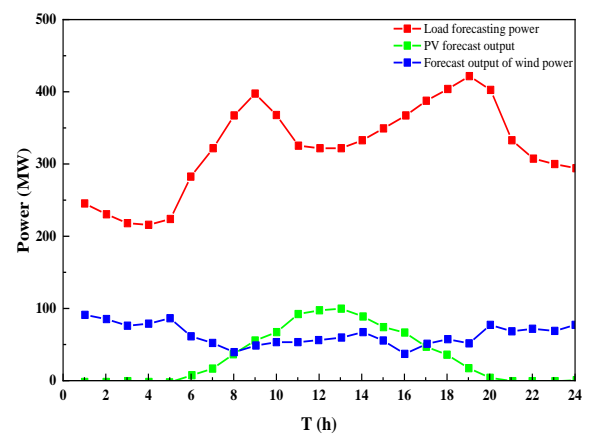


Fig. 3 Forecast Wind and Solar Power Output and Load Forecast for Each Time Period

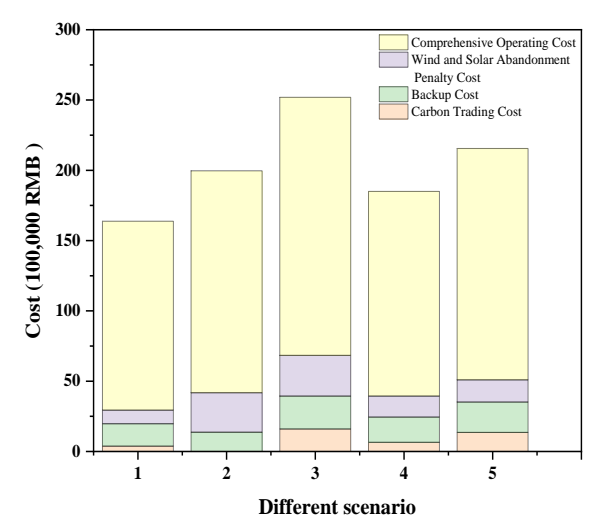


Fig.4 Cost Analysis under Different Scenarios

reserves, five different dispatch scenarios are set up for comparative analysis:

- Scenario 1: The chance-constrained model is used to handle the uncertainties of wind, solar power output, and load, considering carbon trading costs.
- Scenario 2: The chance-constrained model is used to handle the uncertainties of wind, solar power output, and load, without considering carbon trading costs.

- Scenario 3: Carbon trading costs are considered, and traditional spinning reserve capacity methods are used to handle uncertainties.
- Scenario 4: Carbon trading costs are considered, and the
 uncertainties in wind power output and load are handled
 using the chance-constrained model, while the
 uncertainties in solar power output are handled using the
 traditional spinning reserve capacity method.
- Scenario 5: Carbon trading costs are considered, and the uncertainties in solar power output and load are handled using the chance-constrained model, while the uncertainties in wind power output are handled using the traditional spinning reserve capacity method (Liu et al. 2021).

The results of the dispatch planning are shown in Figures 4 and 5. From the perspective of the impact of introducing the carbon trading model on the system, the inclusion of carbon trading costs has a significant effect on overall system costs and carbon emissions (Song *et al.* 2024). Comparing Scenario 1 (with carbon trading costs) and Scenario 2 (without carbon trading costs), we can see that although the total cost of Scenario 1 (1.3435 million yuan) is slightly lower than that of Scenario 2 (1.3793 million yuan), its carbon emissions are more reasonable, at 6,474.68 tons and 7,064.88 tons, respectively. The inclusion of carbon trading costs encourages the system to place greater emphasis on controlling carbon emissions during dispatch, as is also reflected in the performance of Scenario 3 and Scenario 5. For example, although Scenario 3 incorporates carbon trading costs,

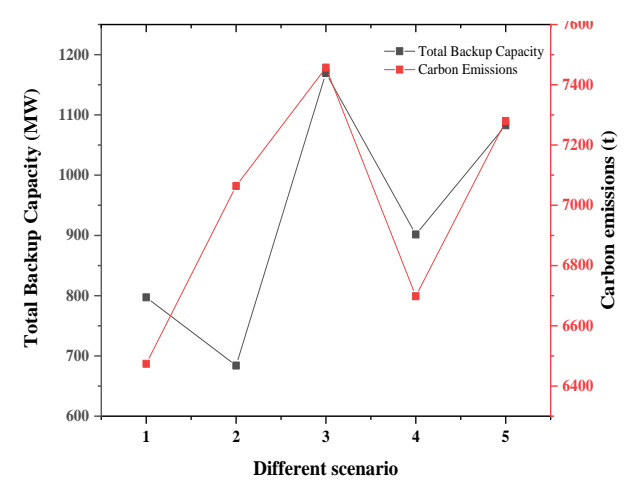


Fig. 5 Reserve Capacity and Carbon Emissions under Different Scenarios

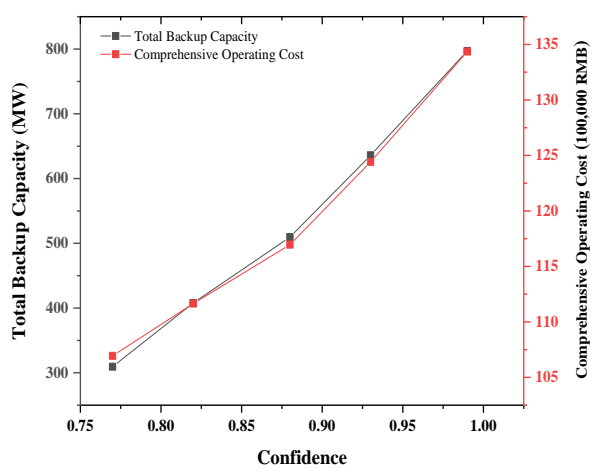


Fig. 6 System Dispatch Results under Different Confidence Levels

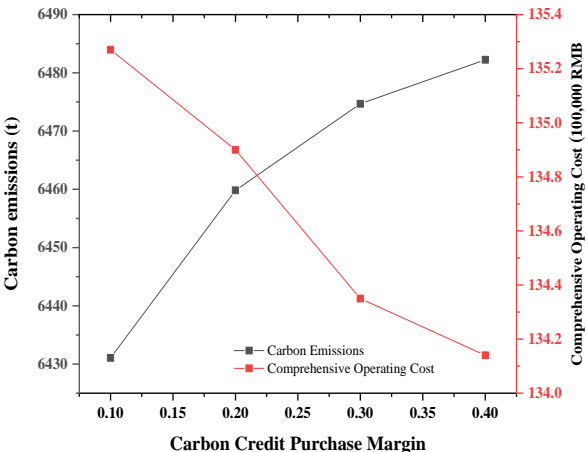


Fig. 7 System Dispatch Results under Different Carbon Credit
Purchase Margins

the total cost is as high as 2.5 million yuan, yet its carbon emissions (7,457.88 tons) are still lower than those in Scenario 2, which does not account for carbon trading. This indicates that while the introduction of the carbon trading mechanism increases economic costs, it effectively limits carbon emissions and enhances the system's environmental benefits (Liu *et al.* 2023). In summary, the inclusion of carbon trading costs promotes lower carbon emissions, but it also imposes a certain financial burden on the system, requiring better dispatch optimization to balance environmental and economic benefits.

Secondly, the introduction of the chance-constrained model shows significant advantages in addressing the uncertainties in wind and solar power output and load. By comparing different scenarios, we can see that in Scenario 1 and Scenario 4 (both using the chance-constrained model), the reserve capacity is 797.14 MW and 901.57 MW, respectively, which are significantly lower than the 1,169.49 MW in Scenario 3 (using the traditional spinning reserve capacity method). This directly reflects the effectiveness of the chance-constrained model in reducing reserve capacity requirements. Moreover, the total costs in Scenario 1 and Scenario 4 are relatively lower, at 1.3435 million yuan and 1.4555 million yuan, respectively, showing an advantage in cost control. In contrast, Scenario 3, which does not incorporate the chance-constrained model, leads to significantly higher reserve capacity and costs, demonstrating that the traditional spinning reserve capacity method introduces excessive redundancy and inefficiency when dealing with uncertainties. Therefore, by more accurately addressing uncertainties, the chance-constrained model significantly reduces reserve capacity requirements, thus lowering system costs and improving overall system operational efficiency (Chen *et al.* 2024).

The system dispatch results corresponding to the sensitivity analysis of different confidence levels and different carbon credit purchase margins are shown in Figure 6 and Figure 7. As shown in Figure 6, with an increase in the confidence level, both reserve capacity and economic costs increase. The confidence level reflects the system's ability to handle the risks associated with supply and demand uncertainties (Li et al. 2024). In the dispatch decision-making process, operators should choose an appropriate confidence level based on the actual needs of the system, balancing safety and economic considerations. As shown in Figure 7, when the carbon credit purchase margin is small, the high penalties for carbon emissions prompt high-cost but low-emission units to increase output, resulting in lower carbon emissions but higher overall costs. As the carbon credit purchase margin increases, the total carbon emissions become smaller than the sum of the carbon quota and the purchased carbon credits, leading to negative penalty costs. This indicates that the excess purchased carbon credits can be sold again, reducing costs. However, when there are no penalty costs, the overall cost increases, and carbon emissions rise accordingly.

In summary, across the five scenarios analyzed, using a stochastic simulation-based chance-constrained model that satisfies both power balance and reserve balance increases system reserve flexibility, avoiding resource waste and reducing system operating costs and carbon emissions. The inclusion of carbon trading costs in the economic dispatch model prioritizes the dispatch of low-carbon and clean energy units. When carbon emissions exceed the set limits, economic penalties are applied. Although costs increase compared to traditional economic dispatch, carbon emissions are significantly reduced. This approach helps power companies better balance economic and environmental impacts, accelerating progress toward the "carbon peak" and "carbon neutrality" goals (Guo et al. 2021).

3.3.2 Comparative Analysis of Different Power Source Integrations

To visually verify the positive effects of different power source integrations on carbon emissions and clean energy utilization, five scenarios were set for comparison:

- Scenario 1: Thermal power output alone.
- Scenario 2: Combined output of solar and thermal power.
- Scenario 3: Combined output of wind and thermal power.

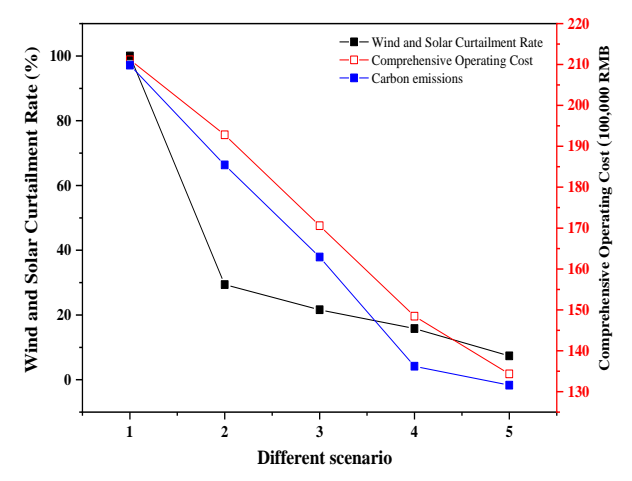


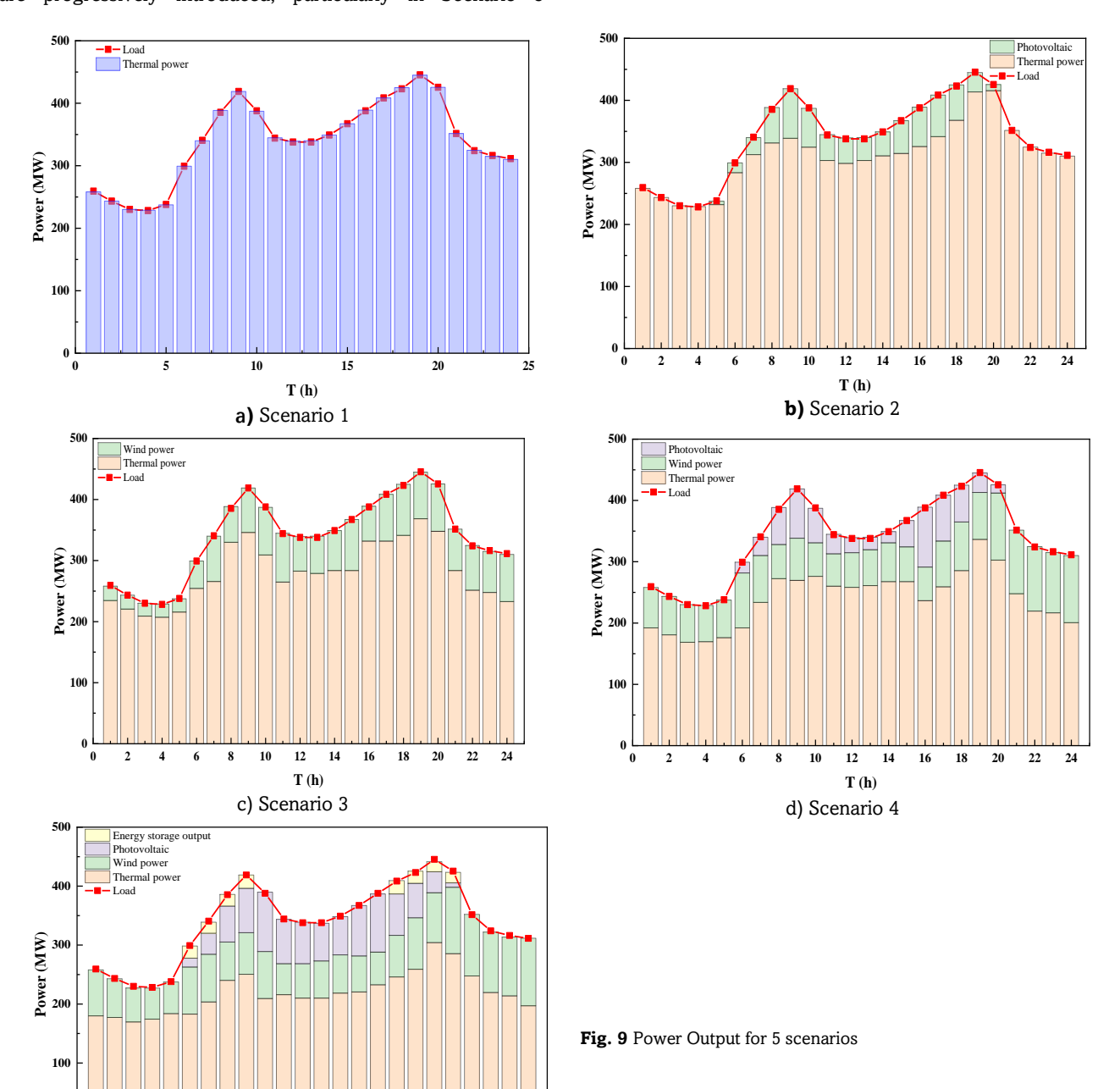
Fig. 8 Dispatch Optimization Results for Different Power Source Integrations

- Scenario 4: Bundled output of wind and solar power combined with thermal power.
- Scenario 5: Combined output of wind, solar, thermal, and energy storage systems.

Figure 8 shows the optimization results of dispatch under different power source integrations. Based on the analysis of the dispatch optimization results in Figure 8, the introduction of renewable energy and energy storage systems significantly r educes the wind and solar curtailment rate, overall costs, and carbon emissions. In Scenario 1, where the system relies solely on thermal power, the wind and solar curtailment rate reaches 100%, the total cost is 2.1114 million yuan, and carbon emissions amount to 9,152.10 tons, the highest among all scenarios. However, as solar, wind, and energy storage systems are progressively introduced, particularly in Scenario 5

10 12 14 T (h) e) Scenario 5 (combined output of wind, solar, thermal, and energy storage systems), the wind and solar curtailment rate drastically drops to 7.37%, the total cost decreases to 1.3434 million yuan, and carbon emissions are reduced to 6,474.69 tons. Compared to Scenario 1, Scenario 5 effectively utilizes clean energy, significantly reducing the reliance on thermal power, lowering fuel consumption and maintenance costs, and mitigating environmental pollution. In Scenario 5, the collaboration between wind and solar power and energy storage not only enhances the efficiency of renewable energy utilization but also improves the overall economic and environmental performance of the system, achieving the optimal dispatch outcome.

Figures 9 illustrates the power output and net load curves of various power sources for Scenarios 1-5. Based on the data from Figures 9.a and 9.b, Scenario 1 relies entirely on thermal



power, with the thermal power output reaching 444.82 MW during peak load periods (such as at the 19th hour), and the lowest output being 228.78 MW, indicating significant fluctuations. The energy consumption and carbon emissions of thermal power are high during system operation. In contrast, Scenario 2 introduces solar power, effectively reducing the pressure on thermal power output during the daytime. For example, at the 9th hour, solar power generation reached 80.09 MW, and the thermal power output dropped from 418.85 MW in Scenario 1 to 338.76 MW, showing the significant relief solar power provides to the thermal power load. However, during nighttime hours when there is no solar power generation, thermal power is still needed to handle most of the load. The highest thermal power output in Scenario 2 is 413.57 MW, slightly lower than the peak in Scenario 1, but still heavily reliant on thermal power to maintain system stability. Overall, Scenario 2 reduces the usage frequency and carbon emissions of thermal power through solar power generation, particularly during daytime peak periods, making system operation more environmentally friendly (Gao et al. 2025). However, thermal power remains indispensable when solar power is unavailable. As shown in Figure 9.c, the addition of wind power significantly alleviates the load pressure on thermal power. During periods of high wind speed (such as the 9th hour), wind power output reaches 72.89 MW, reducing thermal power output from 418.85 MW in Scenario 1 to 345.96 MW, a decrease of about 73 MW. This indicates that wind power can significantly reduce thermal power output during peak periods, thereby reducing carbon emissions and fuel consumption. Compared to Scenario 2 (combined output of solar and thermal power), wind power exhibits greater volatility, resulting in more frequent fluctuations in thermal power output. For example, at the 12th hour, wind power output is 56.60 MW, and thermal power output is 282.71 MW, while in Scenario 2, solar power output is 40.97 MW, and thermal power output is 298.34 MW, with a relatively higher thermal power output. This shows that wind power, compared to solar power, has greater generation capacity and can more effectively reduce the thermal power load. However, during periods of low wind speed (such as from the 1st to the 5th hour), wind power output is low, and thermal power still needs to bear the main load, with output levels similar to those in Scenario 1. This indicates that although wind power can significantly reduce thermal power pressure during high wind speed periods, its intermittency requires thermal power to maintain a high output level during low wind speed periods.

As shown in Figure 9.d, in Scenario 4, the combined output of wind and solar power significantly reduces the load pressure on thermal power. At the 9th hour, wind power output reaches 68.85 MW, and solar power output is 80.43 MW, reducing thermal power output to 269.57 MW, approximately 149 MW lower than the 418.85 MW in Scenario 1, significantly easing the burden on thermal power. Compared to Scenario 2 (combined output of solar and thermal power), Scenario 4 has more stable output during the day due to the addition of wind power, resulting in lower thermal power output. For example, at the 9th hour, thermal power output in Scenario 2 is 338.76 MW, while in Scenario 4 it is 269.57 MW, a reduction of about 69 MW. Additionally, Scenario 4 shows stronger load relief compared to Scenario 3 (combined output of wind and thermal power), as it leverages both wind and solar resources. At the 12th hour, thermal power output in Scenario 3 is 282.71 MW, while in Scenario 4 it is only 258.23 MW, a reduction of about 24 MW. However, during nighttime periods with low wind and solar output, thermal power is still required to bear the main load. For example, at the 24th hour, thermal power output is 200.55 MW,

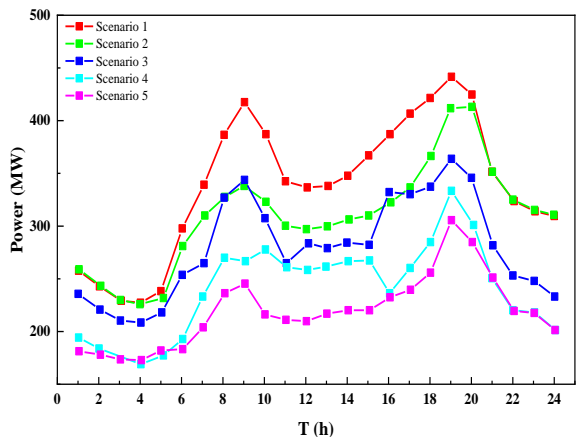


Fig. 10 Net Load Curves under the Five Dispatch Scenarios

which is lower than the 310.10 MW in Scenario 1, but still relatively high. This indicates that the combined output of wind and solar power can significantly reduce the thermal power load during the day, but thermal power is still needed to maintain system stability at night.

As shown in Figure 9.e, compared to the previous four scenarios, Scenario 5, with the combined output of wind, solar, and energy storage, further optimizes the thermal power load, significantly reducing reliance on thermal power. At the 9th hour, wind power output is 70.53 MW, solar power output is 75.28 MW, and energy storage provides 22.58 MW of power support, reducing thermal power output to 250.45 MW. This is a substantial reduction of 168.4 MW compared to the 418.85 MW in Scenario 1, and it is also lower than the 269.57 MW in Scenario 4 and the 345.96 MW in Scenario 3, demonstrating the key role that energy storage plays in stabilizing output. Compared to Scenarios 2 and 3, thermal power output in Scenario 5 is significantly reduced, and energy storage effectively alleviates the load pressure caused by fluctuations in wind and solar output. For example, at the 19th hour, thermal power output in Scenario 5 is 304.12 MW, whereas in Scenario 1 it is as high as 444.82 MW, and in Scenario 4 it is 336.45 MW. This highlights the ability of energy storage to effectively smooth out load fluctuations when wind and solar generation are insufficient. Additionally, during low wind and solar output periods (such as at the 24th hour), thermal power output in Scenario 5 drops to 196.93 MW, compared to 310.10 MW in Scenario 1, indicating that the energy storage system plays a significant role in maintaining stable output during the night. Therefore, with the support of the energy storage system, Scenario 5 further reduces thermal power load fluctuations, achieving more efficient energy dispatch and carbon emissions control.

As shown in Figure 10, with the gradual introduction of renewable energy and energy storage systems, the net load fluctuations of the system are significantly reduced. In Scenario 1 (thermal power output alone), the net load corresponds directly to thermal power output, showing large fluctuations throughout the day, with a net load range from 257.99 MW to 444.82 MW. In Scenario 2, the addition of solar power significantly reduces the daytime net load, particularly at the 9th hour, where it drops to 338.76 MW, demonstrating the alleviating effect of solar power on the thermal power load. In Scenario 3, with the introduction of wind power, the net load decreases to 345.96 MW during periods of sufficient wind resources (such as at the 9th hour), but wind speed fluctuations

cause the nighttime net load to approach that of Scenario 1. In Scenario 4 (combined wind and solar output), the daytime net load is further reduced to 269.57 MW, the lowest daytime net load among all scenarios, though nighttime still relies on thermal power. In Scenario 5, the combined output of wind, solar, and energy storage systems significantly smooths net load fluctuations, with the lowest daytime net load at 250.45 MW, and a relatively low nighttime net load as well (196.93 MW at the 24th hour). The energy storage system effectively mitigates the load pressure caused by wind and solar power fluctuations. Scenario 5 achieves the best dispatch performance, resulting in the lowest net load fluctuations.

4. Conclusion

This study investigates a multi-energy coordinated low-carbon economic dispatch model for wind, solar, thermal, and energy storage systems, considering uncertainties on both the supply and demand sides. A multi-objective optimization method based on a carbon trading mechanism and chance constraints is proposed, aiming to improve the system's low-carbon economic performance and the integration of renewable energy. In the model, a penalizing carbon trading mechanism is introduced to incorporate carbon emission costs into the traditional economic dispatch model, and a stochastic simulation particle swarm optimization algorithm is used to solve the model. The model demonstrates strong adaptability and optimization effects when dealing with the volatility of wind and solar power and load forecasting uncertainties.

The results show that although the introduction of the carbon trading mechanism increases system economic costs, it significantly reduces carbon emissions. For example, in Scenario 1, after introducing the carbon trading mechanism, the total cost increased by 37,300 yuan, but carbon emissions decreased by 8.35%, while wind and solar curtailment penalties decreased by 65.48%, and the overall operating costs were reduced by 14.94%. This demonstrates that the carbon trading mechanism can effectively limit carbon emissions through economic incentives, improving the environmental benefits of the system and promoting the development of low-carbon power systems.

In terms of handling the uncertainties of wind, solar power output, and load, the chance-constrained model shows great flexibility. By setting different confidence levels, the system can flexibly adjust reserve capacity in response to uncertainties. Compared to traditional reserve capacity methods, the scenarios using chance constraints reduced the system's total reserve capacity requirements. For example, the reserve capacity in Scenario 1 decreased by 31.84%, and the overall costs were reduced by 26.83%. This indicates that the chance-constrained model can more effectively manage uncertainties, reduce redundant system configurations, and enhance operational efficiency.

In the scenario analysis with different power sources, as wind, solar, and energy storage systems were gradually introduced, the system's wind and solar curtailment rates, overall costs, and carbon emissions all significantly decreased. For instance, in Scenario 5, the combined output of wind, solar, thermal, and energy storage systems reduced the wind and solar curtailment rate to 7.37%, the overall costs to 1.3434 million yuan, and carbon emissions to 6,474.69 tons. Compared to Scenario 1, which relied solely on thermal power, fuel consumption and carbon emissions were significantly reduced. The energy storage system, through its "energy shifting" function, provided power support during periods of insufficient

wind and solar generation, effectively smoothing the system's load fluctuations and further improving the system's economic and environmental performance.

Overall, the proposed multi-energy coordinated low-carbon economic dispatch model for wind, solar, and thermal systems, incorporating carbon trading mechanisms and chance-constrained optimization, effectively reduces system carbon emissions, reserve capacity requirements, and enhances renewable energy integration. It demonstrates significant economic and environmental benefits. Future research could further explore the role of hydropower and thermal power in balancing base loads and regulating capacity to further enhance low-carbon economic dispatch and achieve sustainable development in power systems.

Acknowledgement: This work is supported by the Science and Technology Project of China Southern Power Grid Company (No. 031900KC23040022)

Author Contributions: Hong Liu: Conceptualization, methodology, formal analysis, writing—original draft, Yongwei Su; supervision, resources, project administration, Kaijing Cai; writing—review and editing, project administration, validation, Yingkang Mo; writing—review and editing, project administration, validation. All authors have read and agreed to the published version of the manuscript.

Conflicts of Interest: The authors declare no conflict of interest.

References

- Aunedi, M., Al Kindi, A. A., Pantaleo, A. M., Markides, C. N., & Strbac, G. (2023). System-driven design of flexible nuclear power plant configurations with thermal energy storage. *Energy Conversion and Management*, 291, 117257. https://doi.org/10.1016/j.enconman.2023.117257
- Chen, L., Zhang, J., Zhang, X., & Liu, H. (2024). A new low-carbon project scheduling problem with renewable and traditional energy: A comprehensive analysis and its solution. *Journal of Cleaner Production*, 143089. https://doi.org/10.1016/j.jclepro.2024.143089
- Elahi Gol, A., & Ščasný, M. (2023). Techno-economic analysis of fixed versus sun-tracking solar panels. *International Journal of Renewable Energy Development*, 12(3), 615-626. https://doi.org/10.14710/ijred.2023.50165
- Gao, C., Lu, H., Chen, M., Chang, X., & Zheng, C. (2025). A low-carbon optimization of integrated energy system dispatch under multisystem coupling of electricity-heat-gas-hydrogen based on stepwise carbon trading. *International Journal of Hydrogen Energy*, 97, 362-376. https://doi.org/10.1016/j.ijhydene.2024.11.055
- Gao, H., Wang, W., He, S., Tang, Z., & Liu, J. (2024). Low-carbon economic scheduling for AIES considering flexible load coordination and multiple uncertainties. *Renewable Energy*, 228, 120643. https://doi.org/10.1016/j.renene.2024.120643
- Gu, H., Li, Y., Yu, J., Wu, C., Song, T., & Xu, J. (2020). Bi-level optimal low-carbon economic dispatch for an industrial park with consideration of multi-energy price incentives. *Applied energy*, 262, 114276. https://doi.org/10.1016/j.apenergy.2019.114276
- Gu, W., Wang, Q., Liu, H., & Desire, W. A. (2023). Multi-energy collaborative optimization of park integrated energy system considering carbon emission and demand response. *Energy Reports*, 9, 3683-3694. https://doi.org/10.1016/j.egyr.2023.02.051
- Guo, Q., Nojavan, S., Lei, S., & Liang, X. (2021). Economicenvironmental evaluation of industrial energy parks integrated with CCHP units under a hybrid IGDT-stochastic optimization

- approach. *Journal of Cleaner Production*, 317, 128364. https://doi.org/10.1016/j.jclepro.2021.128364
- He, Z., Liu, C., Wang, Y., Wang, X., & Man, Y. (2023). Optimal operation of wind-solar-thermal collaborative power system considering carbon trading and energy storage. *Applied Energy*, 352, 121993. https://doi.org/10.1016/j.apenergy.2023.121993
- Huang, Y., Wang, Y., & Liu, N. (2022). Low-carbon economic dispatch and energy sharing method of multiple Integrated Energy Systems from the perspective of System of Systems. *Energy*, 244, 122717. https://doi.org/10.1016/j.energy.2021.122717
- Jin, J., Wen, Q., Cheng, S., Qiu, Y., Zhang, X., & Guo, X. (2022). Optimization of carbon emission reduction paths in the low-carbon power dispatching process. *Renewable Energy*, 188, 425-436. https://doi.org/10.1016/j.renene.2022.02.054
- Jin, J., Wen, Q., Qiu, Y., Cheng, S., & Guo, X. (2023). Distributed robust optimization for low-carbon dispatch of wind-thermal power under uncertainties. *Environmental Science and Pollution Research*, 30(8), 20980-20994. https://doi.org/10.1007/s11356-022-23591-8
- Li, K., Ying, Y., Yu, X., & Li, J. (2024). Optimal Scheduling of Electricity and Carbon in Multi-Park Integrated Energy Systems. *Energies*, 17(9), 2119. https://doi.org/10.3390/en17092119
- Li, Z., Wu, Q., Li, H., Nie, C., & Tan, J. (2024). Distributed low-carbon economic dispatch of integrated power and transportation system. *Applied Energy*, 353, 122134. https://doi.org/10.1016/j.apenergy.2023.122134
- Liu, C., Wang, H., Wang, Z., Liu, Z., Tang, Y., & Yang, S. (2022).

 Research on life cycle low carbon optimization method of multienergy complementary distributed energy system: A
 review. Journal of Cleaner Production, 336, 130380.

 https://doi.org/10.1016/j.jclepro.2022.130380
- Liu, G., Qin, Z., Diao, T., Wang, X., Wang, P., & Bai, X. (2022). Low carbon economic dispatch of biogas-wind-solar renewable energy system based on robust stochastic optimization. *International Journal of Electrical Power & Energy Systems*, 139, 108069. https://doi.org/10.1016/j.ijepes.2022.108069
- Liu, G., Song, X., Liang, T., Li, Y., & Liu, K. (2024). Edge-Cloud Collaborative Optimization Scheduling of an Industrial Park Integrated Energy System. *Sustainability*, 16(5), 1908. https://doi.org/10.3390/su16051908
- Liu, H., Tian, S., Wang, X., Cao, Y., Zeng, M., & Li, Y. (2021). Optimal planning design of a district-level integrated energy system considering the impacts of multi-dimensional uncertainties: A multi-objective interval optimization method. *IEEE Access*, 9, 26278-26289. https://doi.org/10.1109/ACCESS.2021.3053598
- Liu, J., Ma, L., & Wang, Q. (2023). Energy management method of integrated energy system based on collaborative optimization of distributed flexible resources. *Energy*, 264, 125981. https://doi.org/10.1016/j.energy.2022.125981
- Liu, X., Li, X., Tian, J., Yang, G., Wu, H., Ha, R., & Wang, P. (2023). Low-carbon economic dispatch of integrated electricity-gas energy system considering carbon capture, utilization and storage. *IEEE Access*, 11, 25077-25089. https://doi.org/10.1109/ACCESS.2023.3255508
- Luo, Z., Wang, J., Xiao, N., Yang, L., Zhao, W., Geng, J., ... & Dong, C. (2022). Low carbon economic dispatch optimization of regional integrated energy systems considering heating network and P2G. *Energies*, 15(15), 5494. https://doi.org/10.3390/en15155494
- Ma, R., Li, X., Gao, W., Lu, P., & Wang, T. (2020). Random-fuzzy chance-constrained programming optimal power flow of wind integrated power considering voltage stability. *IEEE Access*, 8, 217957-217966. https://doi.org/10.1109/ACCESS.2020.3040382
- Ning, C., & You, F. (2021). Deep learning based distributionally robust joint chance constrained economic dispatch under wind power uncertainty. *IEEE Transactions on Power Systems*, 37(1), 191-203. https://doi.org/10.1109/TPWRS.2021.3096144
- Njie, Y., Wang, W., Liu, L., & Abdullah, .. (2024). Unveiling the Nexus: Analyzing foreign direct investment and energy consumption in shaping carbon footprints across Africa's leading CO2-emitting

- countries. International Journal of Renewable Energy Development, 13(5), 898-908. https://doi.org/10.61435/ijred.2024.60315
- Pandit, M., Chaudhary, V., Dubey, H. M., & Panigrahi, B. K. (2015). Multi-period wind integrated optimal dispatch using series PSO-DE with time-varying Gaussian membership function based fuzzy selection. *International journal of electrical power & energy systems*, 73, 259-272. https://doi.org/10.1016/j.ijepes.2015.05.017
- Prawitasaria, A., Nurliyantia, V., Utamia, D. M. P., & Nurdianaa, E. (2024). A systematic decision-making approach to optimizing microgrid energy sources in rural areas through diesel generator operation and techno-economic analysis: A case study of Baron Technopark in Indonesia. *Int. J. Renew. Energy Dev*, 13, 315-328.https://doi.org/10.61435/ijred.2024.59560
- Rabe, M., Streimikiene, D., & Bilan, Y. (2019). EU carbon emissions market development and its impact on penetration of renewables in the power sector. *Energies*, 12(15), 2961. https://doi.org/10.3390/en12152961
- Song, J., Zhang, Z., Mu, Y., Wang, X., Chen, H., Pan, Q., & Li, Y. (2024). Enhancing environmental sustainability via interval optimization for low-carbon economic dispatch in renewable energy power systems: Leveraging the flexible cooperation of wind energy and carbon capture power plants. *Journal of Cleaner Production*, 442, 140937. https://doi.org/10.1016/j.jclepro.2024.140937
- Takyi, K. N., Gavurova, B., Charles, O., Mikeska, M., & Sampene, A. K. (2024). Assessing the role of circular economy and green innovation in mitigating carbon emissions in the Visegrad countries. *International Journal of Renewable Energy Development*, 13(6), 1149-1161. https://doi.org/10.61435/ijred.2024.60654
- Ting, Q. I. N., Huaidong, L., & Jinqiao, W. A. N. G. (2018). Carbon trading based low-carbon economic dispatch for integrated electricity-heat-gas energy system. *Automation of Electric Power Systems*, 42(14), 8-13. https://doi.org/10.7500/AEPS20171220005
- Wang, C., Lin, X., Nan, J., Feng, J., Zhou, W., & Zhou, H. (2022). Coordinating thermal energy storage capacity planning and multi-channels energy dispatch in wind-concentrating solar power energy system. *Journal of Cleaner Production*, 350, 131405. https://doi.org/10.1016/j.jclepro.2022.131405
- Wang, J., Ren, X., Li, T., Zhao, Q., Dai, H., Guo, Y., & Yan, J. (2024).
 Multi-objective optimization and multi-criteria evaluation framework for the design of distributed multi-energy system: A case study in industrial park. *Journal of Building Engineering*, 88, 109138. https://doi.org/10.1016/j.jobe.2024.109138
- Wang, K., You, D. H., & Pan, K. (2013). Long-term multi-objective optimization dispatch and its evaluation in wind integrated power systems. Advanced Materials Research, 732, 1033-1037. https://doi.org/10.4028/www.scientific.net/AMR.732-733.1033
- Wang, T., Wang, Q., & Zhang, C. (2021). Research on the optimal operation of a novel renewable multi-energy complementary system in rural areas. Sustainability, 13(4), 2196. https://doi.org/10.3390/su13042196
- Wang, Y., Qiu, J., Tao, Y., Zhang, X., & Wang, G. (2020). Low-carbon oriented optimal energy dispatch in coupled natural gas and electricity systems. *Applied Energy*, 280, 115948. https://doi.org/10.1016/j.apenergy.2020.115948
- Wu, G., Hua, H., & Niu, D. (2022). Low-carbon economic dispatch optimization of a virtual power plant based on deep reinforcement learning in China's carbon market environment. *Journal of Renewable and Sustainable* Energy, 14(5). https://doi.org/10.1063/5.0107948
- Yan, N., Ma, G., Li, X., & Guerrero, J. M. (2022). Low-carbon economic dispatch method for integrated energy system considering seasonal carbon flow dynamic balance. *IEEE Transactions on Sustainable Energy*, 14(1), 576-586. https://doi.org/10.1109/TSTE.2022.3220797
- Yang, Y., Qin, C., Zeng, Y., & Wang, C. (2021). Optimal coordinated bidding strategy of wind and solar system with energy storage in day-ahead market. *Journal of Modern Power Systems and Clean*

Energy, 10(1), 192-203. https://doi.org/10.35833/MPCE.2020.000037

Zhan, S., Hou, P., Yang, G., & Hu, J. (2022). Distributionally robust chance-constrained flexibility planning for integrated energy system. *International Journal of Electrical Power & Energy Systems*, 135, 107417. https://doi.org/10.1016/j.ijepes.2021.107417

Zhang, X., Zhang, H., & Yao, J. (2020). Multi-objective optimization of integrated process planning and scheduling considering energy

savings. *Energies*, 13(23), 6181. https://doi.org/10.3390/en13236181

Zhou, Y., Wang, J., Li, Y., & Wei, C. (2023). A collaborative management strategy for multi-objective optimization of sustainable distributed energy system considering cloud energy storage.

Energy, 280, 128183. https://doi.org/10.1016/j.energy.2023.128183



© 2025. The Author(s). This article is an open access article distributed under the terms and conditions of the Creative Commons Attribution-ShareAlike 4.0 (CC BY-SA) International License (http://creativecommons.org/licenses/by-sa/4.0/)